A New Load Adaptive Identification Method Based on an Improved Sliding Mode Observer for PMSM Position Servo System

Wenqi Lu, Bo Tang, Kehui Ji, Kaiyuan Lu, *Member, IEEE*, Dong Wang, *Member, IEEE*, and Zhijun Yu

***Abstract*—The effective identification of the load torque is one of the key methods to improve the positioning accuracy of the position servo system, and the sliding mode observer (SMO) is a common identification method in the speed control system because of its advantages of insensitive parameters and easy physical realisation. However, the existing SMO cannot achieve high precision and high response identification of load torque in the full speed range when the motor is running at variable-speed or variable-load, which limits its application in the position servo system. Based on the analysis of the stability and the adaptive law of feedback gain coefficient, an improved SMO for adaptive identification based on adaptive control and improvement of cut-off frequency is proposed. To verify the proposed method, the dedicated simulation model and test platform are built. The results show that the proposed observer can realize the adaptive identification of the load torque under the condition of variable-speed or variable-load, and the estimation accuracy is high. The position servo system designed by the proposed observer can improve the response against load change, which is an effective method for high-precision positioning control of the position servo system with a variable-speed or variable-load.**

***Index Terms*—Adaptive identification, high-precision positioning, improved sliding mode observer (SMO), position servo system.**

I. Introduction

THE high-speed and high-precision position servo system is one of the key technologies for the research and development of the mechanical arm such as welding robot, double arm cooperation robot, etc. For this, in recent years, some methods have been put forward to suppress the changes of internal electric parameter or external mechanical disturbance. This article summarizes and classifies these methods, which can be divided into the following two categories: one is the method of changing the original three-loop proportion integration differentiation (PID) control structure, such as autodisturbance rejection observer [1], [2], internal model control [3], [4], two degrees of freedom PID control [5], [6], etc. The characteristic of this kind of method is that the controller is not specially designed to suppress a certain parameter change or disturbance, but it is effective to suppress a variety of parameter changes or disturbances. Generally, it does not involve the self-tuning of the controller parameters, which can improve the response speed, robustness and positioning accuracy of the servo system to a certain extent. However, this method not only needs to adjust more parameters of the controller but also has the problem of difficult parameter setting. Moreover, the time delay characteristic of the controller will produce overshoot and deviation for the positioning of the large inertia load system such as the manipulator, which is more suitable for the application of the small inertia load object. For example, in [1] and [2], it adopted active disturbance rejection control (ADRC) to realize the control of robustness and immunity of motor parameters. However, the ADRC controller has many settings, and it adopted multiple ADRC controllers, which cause parameters tuning is more complicated.

Another is parameter self-tuning method based on traditional PID control structure, which can also be divided into two main categories: the PID self-tuning method based on intelligent control [7]–[9], and the PID parameter self-tuning method based on modern control theory [10]–[21]. Among them, the PID parameter self-tuning method based on intelligent control generally uses fuzzy control or neural network to solve the uncertainty problem [7]–[9], the deviation between the actual output and the expected output is used as the basis for parameter change. When the deviation is eliminated, the parameter tuning ends. However, it ignores the periodicity of the setting process and the self-learning ability, which results in low efficiency and long positioning time. The PID parameter self-tuning method based on modern control theory mostly adopts the targeted method of first identifying disturbance and then compensating or adjusting controller parameters. The time of parameter tuning is only limited by the response time of parameter identification. As long as time is short, the tuning efficiency of the system will be very high. Its implementation process can be summarized as "(parameter) identification-adjustment (compensation)-adaptation".

Manuscript received March 18, 2020; revised July 5, 2020; accepted August 5, 2020. Date of publication August 14, 2020; date of current version October 30, 2020. This work was supported in part by the Zhejiang Provincial Natural Science Foundation of China under Grants LY18E070006 and LY19E070006, in part by the National Natural Science Foundation of China under Grant 51677172, and in part by the Fundamental Research Funds of Zhejiang Sci-Tech University under Grant 2019Q031. Recommended for publication by Associate Editor T. Shi. *(Corresponding authors: Wenqi Lu; Kaiyuan Lu.)*

Wenqi Lu, Bo Tang, and Kehui Ji are with the Faculty of Mechanical Engineering and Automation, Zhejiang Sci-Tech University, Hangzhou 310018, China (e-mail: luwenqi@zstu.edu.cn; tangbok@163.com; jkh@zstu.edu.cn).

Kaiyuan Lu and Dong Wang are with the Department of Energy Technology, Aalborg University, 9220 Aalborg, Denmark (e-mail: klu@et.aau.dk; dwa@et.aau.dk).

Zhijun Yu is with Jiangsu Yuandong Electric Manufacturing Company, Ltd., Taizhou 225500, China (e-mail: zhhbyyzj@126.com).

Color versions of one or more of the figures in this article are available online at https://ieeexplore.ieee.org.

Digital Object Identifier 10.1109/TPEL.2020.3016713

At present, it is the main method to restrain parameter change or disturbance, and the effective identification of the load torque is the key foundation of this method.

For the identification of the load torque, many methods have been proposed. In [10] and [11], a full/reduced-order observer is proposed, and it is applied to the case of heavy load driving, such as servo broaching machine, servo press, etc. But, the calculation accuracy depends on the motor parameters, which are not suitable for the complex system. In [12] and [13], an adaptive control strategy based on a disturbance observer is proposed. The disturbance observer is used to estimate the load change, and the adaptive controller is used to compensate for the norm bounded disturbance, which effectively improves the anti-interference ability. But, these methods are still dependent on the mathematical model of the motor and have low robustness to parameter changes. In [14] and [15], the load torque observer based on a Kalman filter is proposed, and the simulation and experimental verification are carried out. The results show that the method can achieve excellent results, but these observers are more complex, which are difficult to be applied in the large inertia load system such as the mechanical arm. In [16]–[18], the model reference adaptive control method is used to identify the load torque, and the experimental results verify the validity of the method. However, these methods also depend on the motor parameters and have low robustness.

The sliding mode variable structure control has been introduced to the identification algorithm of load torque by researchers due to its insensitivity to parameter change and disturbance, fast response, and easy physical realization. For example, in [20], a sliding mode observer is introduced into the identification of load torque for the first time. The load torque and speed are taken as the state variables, and the deviation between the actual value and the observed value of speed is considered as the sliding mode switching surface. The switching signal is designed by the sign function. Theoretical analysis and experiments show that the observer can accurately observe the load torque. However, the two variables of load torque and speed are used as state variables in the observer, and the calculation process is complex; the switch function is used as switching function, which has the problems of chattering, low accuracy of load torque identification, slow response and so on. In order to solve this problem, a new load torque identification sliding mode observer is proposed in [21]. The switching function is replaced by saturation function, and the estimated load torque feedback is introduced into the speed observation mathematical model of the traditional sliding mode observer. The results show that the new sliding mode observer for load moment identification has higher accuracy and faster response than the traditional observer. It is an effective method for load moment identification and disturbance suppression. However, at present, this method is researched based on a servo system with constant speed and constant load using the method of adjusting compensation and optimizing control parameters manually. When the system is running at variable-speed or variable-load, such as the position servo drive system of robot joints, it is necessary to make an offline table for the control parameter and compensation quantity according to the test results and use the offline table to adjust the observer parameters, but the offline table data often depends on the system parameters and the resource allocation of the control core, which limits the application of this method in the high-speed and high-precision position servo system.

Therefore, in order to realize the adaptive identification of load torque under the condition of variable-speed or variable-load for the high-precision positioning of the position servo system, an improved sliding mode observer for adaptive identification based on adaptive control and improvement of cut-off frequency is proposed. The theoretical analysis and experimental test are carried out, which are described below.

II. Proposed Improved Sliding Mode Observer for the Load Torque Identification

In order to solve the problem of load disturbance compensation in the high-speed and high-precision position servo system, an improved load torque identification sliding mode observer is proposed based on the design idea of "(parameter) identification-adjustment (compensation)-adaptation" as mentioned earlier, which can adaptively estimate the load torque during the variable-speed and variable-load operation. Its principle is described later.

A. Design of the Traditional Load Torque Identification Sliding Mode Observer

The voltage equation of the permanent magnet synchronous motor (PMSM) in the *d–q* two-phase coordinates is

$$\begin{cases} u_d = Ri_d + L_d di_d/dt - \omega_e L_q i_q \\ u_q = Ri_q + L_q di_q/dt + \omega_e (L_d i_d + \psi_f). \end{cases} \tag{1}$$

The torque equation of PMSM is

$$T_e = 1.5P_n \left[\psi_f i_q - (L_q - L_d) i_d i_q\right]. \tag{2}$$

The motion equation of PMSM is

$$(J/P_n) d\omega_e/dt = T_e - B\omega_e/P_n - T_L \tag{3}$$

where R is stator resistance; u_d, u_q, i_d, i_q, L_d, and L_q are the stator d-axis and q-axis voltages, currents, inductances, respectively; ψ_f is the rotor permanent magnet flux-linkage; J is the moment of inertia; B is the viscous friction coefficient; P_{n} is the number of pole-pairs; ω_e is the electrical actual angular velocity of the motor; T_e and T_L are the electromagnetic torque and load torque, respectively.

By substituting (2) into (3), the state equation of PMSM can be obtained as

$$\begin{aligned} d\omega_e/dt = {} & 1.5P_n^2[\psi_f i_q + (L_d - L_q) i_d i_q]/J \\ & - P_n T_L/J - B\omega_e/J. \end{aligned} \tag{4}$$

In [21], a traditional sliding mode observer is proposed, in which the saturation function replaces the sign function, and the estimated load torque is introduced into the mathematical model of the speed observer. Based on this, the speed estimation

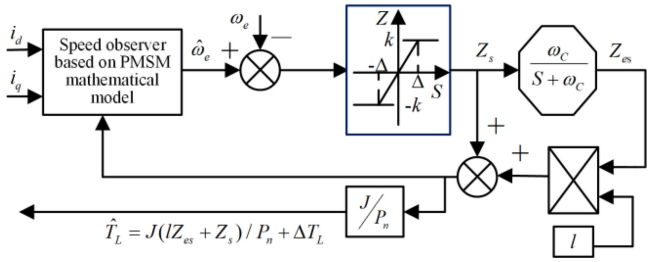

Fig. 1. Schematic diagram of the traditional load torque identification SMO.

formula of the traditional sliding mode observer is obtained as follows:

$$d\hat{\omega}_e/dt = 1.5P_n^2[\psi_f i_q + (L_d - L_q)i_d i_q]/J - lZ_{\rm es} - B\hat{\omega}_e/J - Z_{\rm s} \quad (5)$$

where $Z_s = k \times sat(\hat{\omega}_e - \omega_e)$ is the saturation function, l is the feedback gain coefficient of Z_{es}, Z_{es} is the equivalent control function, as shown in (6), which is obtained by filtering the control function Z_s with a low-pass filter

$$Z_{es} = Z_s \times \omega_c/(s+\omega_c). \quad (6)$$

In (6), ω_c is the cut-off frequency of the low-pass filter.

Defining the speed estimation error as $\tilde{\omega}_e = \hat{\omega}_e - \omega_e$ it can be obtained by subtracting (4) from (5) that

$$d\tilde{\omega}_e/dt = P_n T_L/J - lZ_{\rm es} - B\tilde{\omega}_e/J - Z_{\rm s}. \quad (7)$$

According to the sliding mode control theory, the sliding surface is defined as

$$S(x) = \tilde{\omega}_e = \hat{\omega}_e - \omega_e = 0. \quad (8)$$

It satisfies $S_s{=}\dot{S}_s{=}0$ when the system enters the steady-state and sliding around the sliding mode surface. Thus, the load torque can be estimated as

$$\hat{T}_{sL}{=}J(lZ_{\rm es}{+}Z_{\rm s})/P_n. \quad (9)$$

It can be seen from (9) that the load torque identification $\hat{T}_{sL}$ is composed of two parts: $J(lZ_{es})/P_n$ and $J(Z_s)/P_n$, respectively. Among them, the $J(Z_s)/P_n$ retains the harmonic component caused by the switching function Z_s, and the $J(lZ_{es})/P_n$ contains the effective components after the harmonic content is filtered. The calculation of $J(lZ_{es})/P_n$ will inevitably introduce response delay and estimation error. When running at variable-speed or variable-load, it must be compensated, and the compensation quantity is directly related to the phase response of the low-pass filter, which can be obtained according to

$$\Delta T_L = \tan^{-1}(\omega_{T_L}/\omega_c) \quad (10)$$

where ω_{T_L} is the frequency of estimated load torque.

Based on the above analysis, the schematic diagram of the traditional load torque identification SMO (old_SMO) can be obtained, as shown in Fig. 1.

To estimate the load torque accurately, [21] has carried out experiments on the constant speed and constant load system with manual adjustment of the compensation quantity ΔT_L and the optimization of the l parameter, as shown in Fig. 1, which realizes the accurate identification of load torque under the condition of constant speed and constant load. However, when the system is running at periodically variable-speed or variable-load condition, it is necessary to make an offline table for the l parameter and compensation quantity according to (10) and use the offline table to adjust the observer parameters. But, the offline table data often depends on the system parameters and the resource allocation of the computer control core, which limits its practical engineering application.

B. Design of the Improved Load Torque Identification Sliding Mode Observer

In order to solve the problems of the traditional sliding mode observer mentioned above in the case of variable-speed or variable-load, first, a low pass filter with the cut-off frequency changing with the ω_{T_L} is proposed as

$$H(j\omega_{T_L}) = \omega_c/(j\omega_{T_L} + \omega_c)$$
$$\omega_c = \begin{cases} \omega_{T_L}/{\rm M}\ \omega_{T_L} > \omega_{T_{L1}} \\ \omega_{T_{L1}}/{\rm M}\ \omega_{T_L} \le \omega_{T_{L1}}. \end{cases} \quad (11)$$

In (11), M is a constant coefficient (general 0.2∼0.5).$\omega_{T_{L1}}$ is the lowest cut-off frequency, corresponding to the minimum frequency threshold of the load torque, to prevent zero denominators when the load torque and speed are constant. Since the value $\omega_{T_{L1}}$ is small, the compensation quantity can be calculated by

$$\Delta T_L = \tan^{-1}(\omega_{T_L}/\omega_c) = \tan^{-1}M. \quad (12)$$

Then, the final estimation formula of load moment can be obtained as follows, according to (6), (9), and (12):

$$\hat{T}_L = \hat{T}_{sL} + \Delta T_L = J(l{+}1{+}s/\omega_c)Z_{\rm es}/P_n + \tan^{-1}M$$
$$= J(l{+}1{+}jM)Z_{\rm es}/P_n + \tan^{-1}M \quad (13)$$

where $s = j\omega_{T_L}$.

It is known from (10)–(12) that the cut-off frequency of the low pass filter varies with the frequency of estimated load torque, and the offset of estimated load torque is a constant associated with the constant *M*. In this way, the cut-off frequency and compensation quantity of the low-pass filter can be calculated based on the estimated load torque and constant *M*. Thus, the accurate load torque can be estimate conveniently. It is known from (13) that the response delay of the load torque identification value is caused by the introduction of the low-pass filter and parameters l. If $l = 0$, it is the sliding mode observer with the saturation function. The delay of the load torque identification value is determined only by the introduction of the low-pass filter. If $l \neq 0$, the introduction of l increases the phase lag effect of the original low-pass filter when $-1 < l < 0$; the introduction of l weakens the phase lag effect of the original low-pass filter when $l > 0$, and the larger the l is, the smaller response delay is. In this way, the disturbance and harmonic of the load torque estimation can be effectively balanced by adding the feedback coefficient l to the compensation of the original low-pass filter, thus improving the estimation accuracy.

Second, according to the sliding mode variable structure control principle and the proposed low-pass filter, an adaptive control method of the feedback gain coefficient is proposed.

The condition for the existence of the sliding mode is

$$V = S \times \dot{S} < 0. \tag{14}$$

By substituting (4), (7), and (8) into (14), it can be obtained that

$$S \times \dot{S} = \begin{cases} \left[P_n T_L/J - \left(1 + l\omega_c/\left(j\omega_{T_L} L + \omega_c\right)\right) k\right] S - BS^2/J \\ \qquad\qquad S > \Delta \\ \left[P_n T_L/J - \left(1 + l\omega_c/\left(j\omega_{T_L} + \omega_c\right)\right) kS/\Delta\right] S - BS^2/J \\ \qquad\qquad -\Delta < S < \Delta \\ \left[P_n T_L/J + \left(1 + l\omega_c/\left(j\omega_{T_L} + \omega_c\right)\right) k\right] S - BS^2/J \\ \qquad\qquad S < -\Delta. \end{cases} \tag{15}$$

Because $-BS^2/J < 0$, $-(1 + l\omega_c/(j\omega_{T_L} + \omega_c))kS^2/\Delta < 0$, it can be seen from the analysis that if (16) is established and substituted into (15), then (15) satisfies the condition of (14). Therefore, (16) is the necessary condition for the stability of the sliding mode observer

$$\left(1 + l\omega_c/\left(j\omega_{T_L} + \omega_c\right)\right) k > P_n T_L/J. \tag{16}$$

By substituting (11) into (16), it can be obtained that

$$l > \left(P_n T_L/(k \times J) - 1\right)(jM + 1). \tag{17}$$

In order to satisfy the relationship of formula in (17) and simplify the calculation, M in (17) is removed, and (17) can be simplified as

$$l > \left(P_n T_L/(k \times J) - 1\right). \tag{18}$$

The selection of feedback gain coefficient l must satisfy the stability requirement of (18); otherwise, the observer cannot perform sliding mode motion. According to (18), the value of the feedback gain coefficient l is proposed as

$$l = 2P_n T_{Ln}/kJ - 1 \tag{19}$$

where T_{Ln} is the maximum load torque of the motor.

By substituting l into (13), it can be obtained that

$$\begin{aligned} \hat{T}_L &= J\left\{jM + 2P_n T_{Ln}/kJ\right\} \times Z_{es}/P_n + \tan^{-1} M \\ &\approx 2T_{Ln} \times Z_{es}/k + \tan^{-1} M. \end{aligned} \tag{20}$$

According to (19) and (20), the schematic diagram of the proposed improved load torque identification SMO (new_SMO) can be obtained, as shown in Fig. 2.

C. Stability Analysis

The proposed improved load torque identification SMO described in (7) is used for stability analysis.

When $S > \Delta$, the output signal of the saturation function is constant k (i.e., $Z_s = k$), so as the output of the low pass filter (LPF) (i.e., $Z_{es} = k$). Similarly, for condition $S < -\Delta$, it has $Z_s = Z_{es} = -k$. When the SMO is operating around the sliding

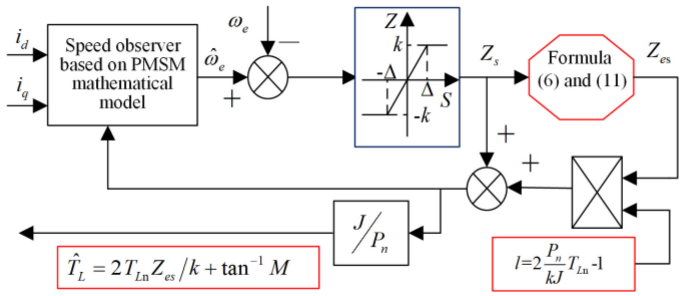

Fig. 2. Schematic diagram of the proposed improved load torque identification SMO.

surface (i.e., $-\Delta < S < \Delta$), supposing the cut-off frequency of the LPF is high, and the effective signal of S (i.e., not including the noise) is not affected, it has $Z_s = Z_{es} = S \cdot k/\Delta$. Then, (7) can be rewritten as where the sliding surface S is the speed error as defined in (8)

$$\frac{dS}{dt} + \frac{B}{J}S - \frac{P_n}{J}T_L = \begin{cases} -k\,(1+l)\,, & S > \Delta \\ -\frac{k}{\Delta}S(1+l), & -\Delta < S < \Delta \\ k\,(1+l)\,, & S < -\Delta. \end{cases} \tag{21}$$

According to the Routh–Hurwitz stability criterion, when $S > \Delta$ or $S < -\Delta$, the system is stable if B/J> 0, which is always true; when $-\Delta < S < \Delta$, the system is stable if $B/J+(1+l)\cdot k/\Delta > 0$, which is always held as well since all the parameters have positive values. The larger the coefficient $B/J+(1+l)\cdot k/\Delta$ value is, the larger the system damping factor becomes, and the shorter the system transient is.

If taking the influence of the LPF into consideration when the speed error varies around the sliding surface, i.e., $-\Delta < S < \Delta$, the system equation in the frequency domain can be expressed as

$$s\tilde{\omega}_e + \frac{B}{J}\tilde{\omega}_e - \frac{P_n}{J}T_L = -\frac{k}{\Delta}\tilde{\omega}_e\left(1 + l \cdot \frac{\omega_c}{s + \omega_c}\right) \tag{22}$$

where s is the complex variable of Laplace transform, and $\tilde{\omega}_e$ is used to replace s to avoid possible confusion. By rewriting (21), it can be obtained that

$$\begin{aligned} s^2\tilde{\omega}_e + \left(\omega_c + \frac{B}{J} + \frac{k}{\Delta}\right)s\tilde{\omega}_e \\ + \omega_c\left(\frac{B}{J} + \frac{k}{\Delta}(1+l)\right)\tilde{\omega}_e = \frac{P_n}{J}\left(\dot{T}_L + \omega_c T_L\right) \end{aligned} \tag{23}$$

where $\dot{T}_L$is the time derivative of T_L. According to Routh–Hurwitz stability criterion, the system is stable if $(\omega_c + \frac{B}{J} + \frac{k}{\Delta}) > 0$ and $\omega_c(\frac{B}{J} + \frac{k}{\Delta}(1+l)) > 0$, which is always true for the proposed SMO. It can be seen from the above analysis that the proposed SMO is always stable, which is a big advantage.

III. Design of the Position Servo System

The schematic diagram of the position servo system is shown in Fig. 3, which is composed of position control loop based

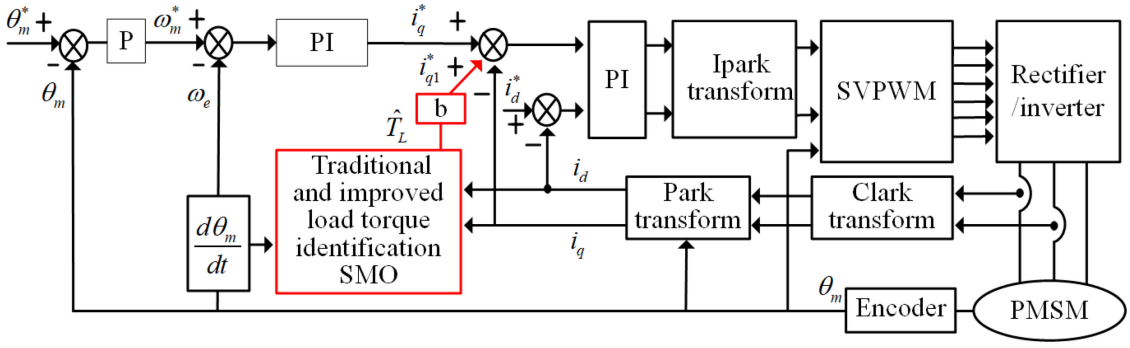

Fig. 3. Schematic diagram of the position servo system.

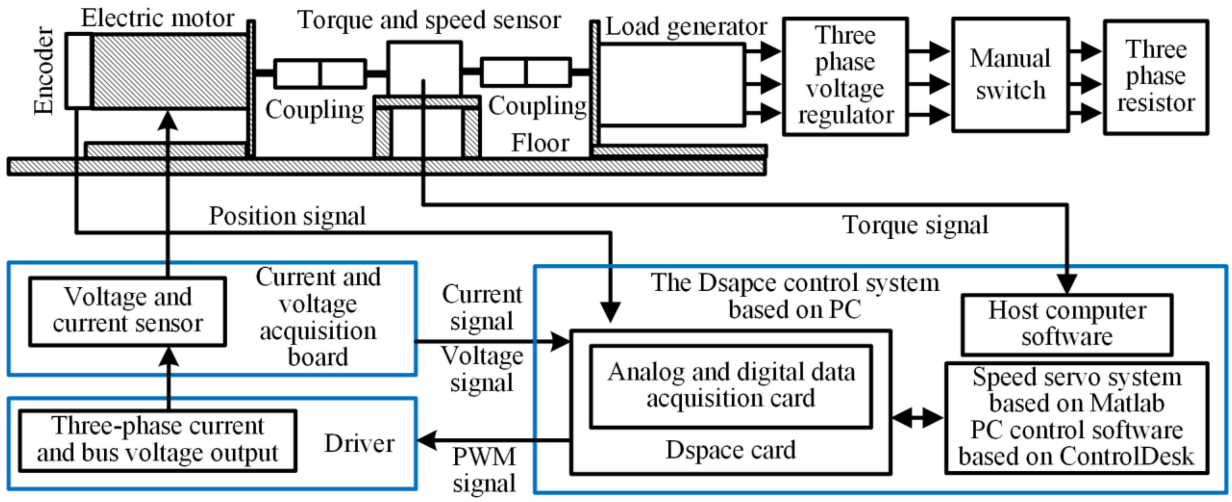

Fig. 4. Schematic diagram of the special motor driving test platform.

on a *P* regulator, speed control loop based on a proportion integration (PI) regulator, current control loop based on a PI regulator, Park transform, Ipark transform, Clark transform, rectifier/inverter, encoder, PMSM, space vector pulsewidth modulation (SVPWM), traditional and improved load torque identification SMO, etc. Among them, the load torque identification SMO (as shown in Figs. 1 and 2) is used for estimating the load torque. The identification value of the load torque is feed-forward compensated to the given end of the quadrature current, where *b* is the feed-forward coefficient. And, *b* is set according to the torque coefficient of the motor.

IV. Experimental Test

In order to verify the correctness and superiority of the proposed scheme, a simulation model of position servo system and a special motor driving test platform are designed, whose special feature is that the load is a function of speed. The schematic diagram of the motor driving test platform is shown in Fig. 4, which is composed of a prime motor (PMSM), encoder, torque-speed sensor, load generator (PMSM), three-phase voltage regulator, manual switch, three-phase resistor, driver, current and voltage acquisition board, DSpace control system based on PC, etc. The actual platform based on Fig. 4 is shown in Fig. 5, and the main parameters are given in Table I.

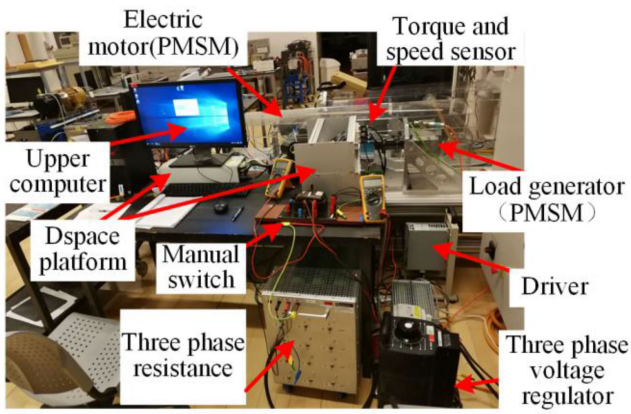

Fig. 5. Motor dragging test platform based on DSpace.

A. Test of the Estimated Performance of the Old_ SMO

The performance of the Old_SMO is carried out at a given constant speed of 500 and 2000r/min, respectively, with a given

TABLE I
KEY PARAMETERS OF THE SPECIAL MOTOR DRIVING TEST PLATFORM

Electric motor (PMSM)		Other key parameters	
Rated speed (rpm)	2000	Load generator (PMSM)	SIEMENS 1FK7080
Rated torque (N.m)	6	Torque and speed sensor	DR-3000
Polar logarithm	4	DSpace platform	DS1103
Resistance(Ω)	0.68	M	0.2
Q-axis and d-axis inductor (mH)	0.0055		
Total moment of inertia (kg.m^2)	0.01482		
Rated voltage (V)	380		

constant load torque of half and full load, respectively, as shown in Fig. 6. It can be seen from Fig. 6(a) that compared with the average load torque of 2.98 N.m at 500 r/min, the maximum ripple of the actual load torque, estimated load torque obtained by old_SMO is 0.27% and 0.97%, respectively, when $l = 5$, $\Delta = 20$, and $k = 500$. It can be seen from Fig. 6(b) that compared with the average load torque of 6.05 N.m at 500 r/min, the maximum ripple of the actual load torque, estimated load torque obtained by old_SMO are 0.20% and 0.46%, respectively, when $l = 8$, $\Delta = 20$, and $k = 800$. It can be seen from Fig. 6(c) that compared with the average load torque of 2.98 N.m at 2000 r/min, the maximum ripple of the actual load torque estimated load torque obtained by old_SMO is 1.88% and 2.01%, respectively, when $l = 10$, $\Delta = 20$, and $k = 800$. It can be seen from Fig. 6(d) that compared with the average load torque of 6.05 N.m at 2000 r/min, the maximum ripple of the actual load torque, estimated load torque obtained by old_SMO are 0.86% and 1.74%, respectively, when $l = 15$, $\Delta = 20$, and $k = 1000$.

Therefore, it can be concluded from the experimental results that the estimated load torque value can be obtained from the old_SMO under different values of l,Δ,k, which is not suitable for the operating conditions of varying speed and load.

B. Comparative Test of the Estimated Performance

In order to verify the correctness of the proposed method and its superiority in the case of variable-speed and variable-load, a comparative test is carried out under the condition that the given speed is a square wave curve which changes between 0-2000 r/min, when $l = 15$, $\Delta = 20$, and $k = 1000$ is used in old_SMO. The actual load is a function of speed which is realized based on the three-phase voltage regulator and three-phase resistor. The full load is set through adjusting the voltage value of the three-phase voltage regulator and the resistance value of the three-phase resistance when the motor is running at the maximum speed in steady state.

The actual speed and estimated speed waveforms obtained by the encoder, traditional sliding mode observer, and proposed sliding mode observer are shown in Fig. 7(a), respectively. It can be seen from the waveform that the estimated speed can well follow the change of the actual speed when the actual speed

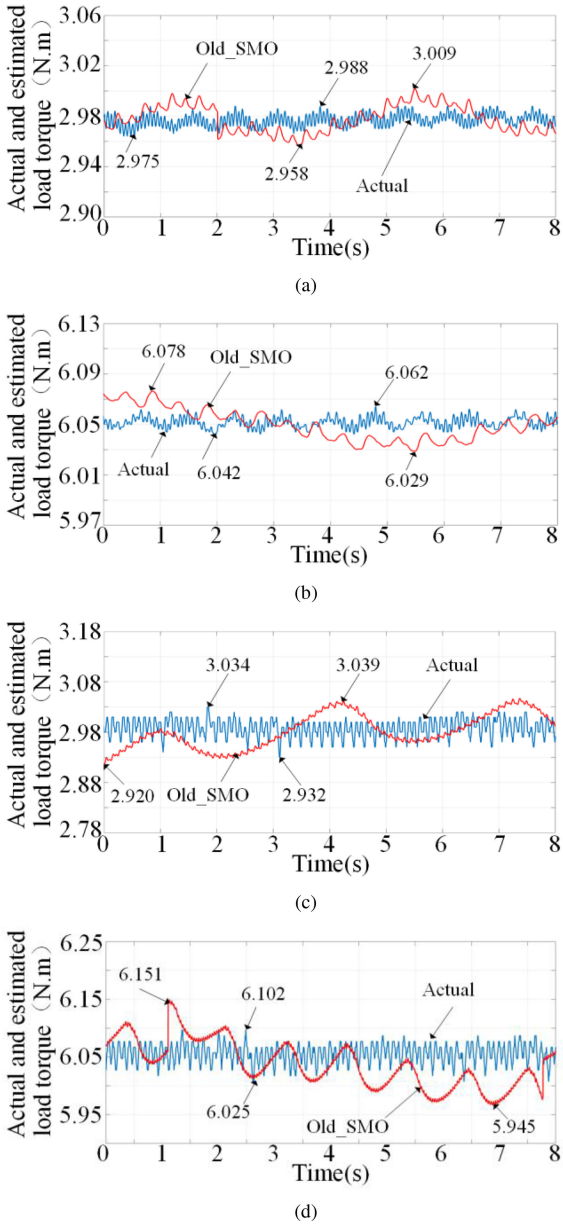

Fig. 6. Load torque estimation performance comparison. (a) 500 r/min with half load torque (3 N.m). (b) 500 r/min with full load torque (6 N.m). (c) 2000 r/min with half load torque. (d) 2000 r/min with full load torque.

changes. The tracking performance of the new_SMO is slightly better than that of old_SMO when the actual speed is 2000 r/min. The estimated speed of the new_SMO is 2001 r/min, which is 1996 r/min from the old_SMO; when the actual speed is 0 rpm, the estimated speed of the new_SMO is 6 r/min and, which is 14 r/min from the old_SMO. Therefore, the estimated speed performance of the new_SMO is better than that of Old_SMO.

The actual load torque and the estimated load torque obtained by the torque-speed sensor, traditional sliding mode observer and proposed sliding mode observer are shown in Fig. 7(b), respectively. It can be seen from the waveforms that the actual load torque varies with the actual speed of the motor in the process of acceleration and deceleration.

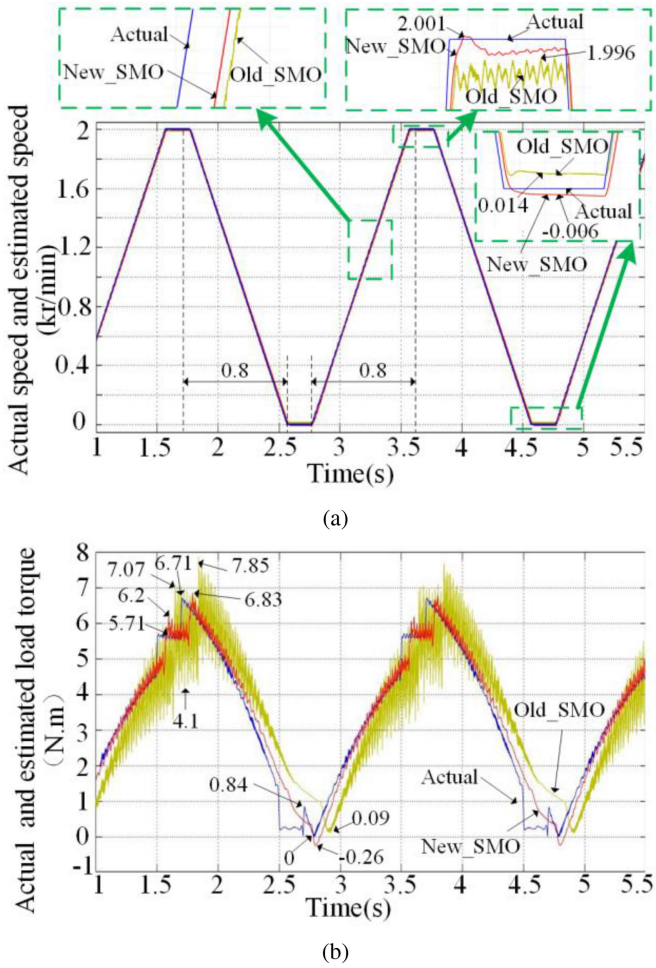

Fig. 7. Test under the condition that the given speed is 0–2000 r/min and the actual load is a function of speed. (a) Actual and estimated speed. (b) Actual and estimated load torque.

The estimated load torque obtained by the traditional sliding mode observer can vary with the change of the actual load torque. However, the optimal compensation of chattering and delay is realized by manually adjusting the parameter l and the compensation amount at different speeds. According to the waveform in Fig. 7(b), a group of optimized combination parameters are set at the speed of 600 r/min, and the chattering and delay are both small. But, when the system is running at variable speed, the chattering of estimated load torque increases with the increase of actual speed, and the delay also occurs with the change of actual speed. Especially in 2000 r/min steady-state operation, the maximum steady-state error of the estimated value is 28.2%.

The estimated value of the load torque obtained by the new sliding mode observer can also change with the actual load torque. But because of the adaptive control and improvement of the cut-off frequency proposed in this article, the chattering and dynamic response performance of the estimated load torque is significantly better than that of the traditional sliding mode observer, and the maximum steady-state error of the motor at 2000 r/min is also small (8.6%).

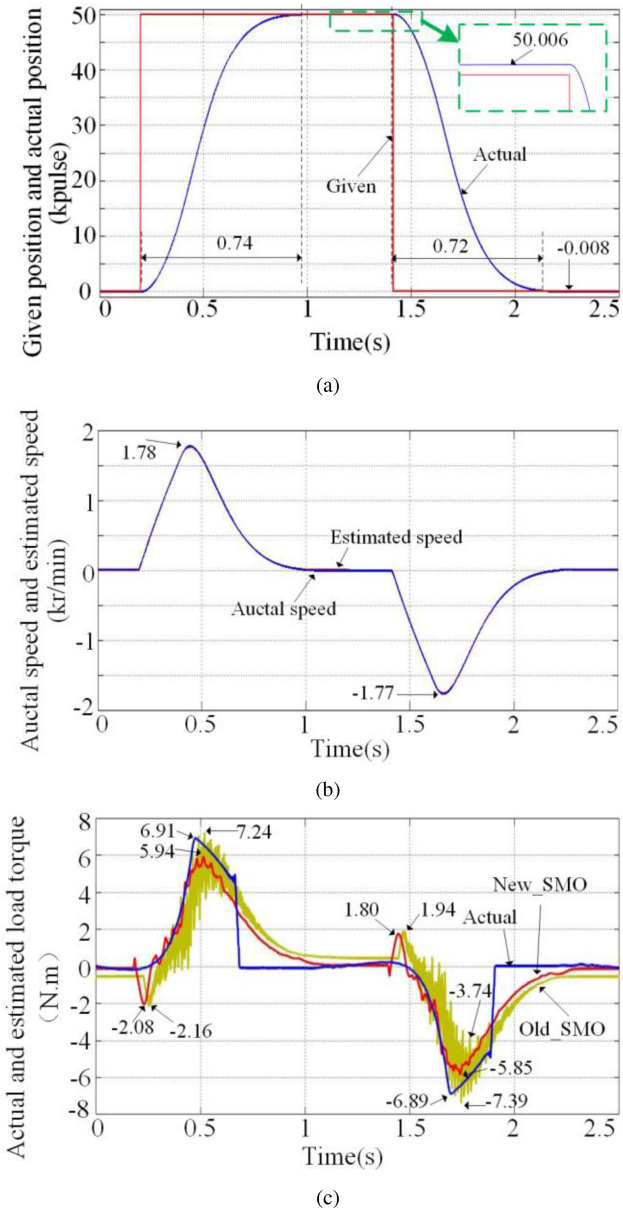

Fig. 8. Test under the condition that the given pulse is 0–50 000 and the actual load is a function of speed. (a) Given and actual position. (b) Actual and estimated speed. (c) Actual and estimated load torque.

Second, in order to further verify the superiority of the proposed method in the positioning process. In this article, two kinds of the sliding observer are tested again under the condition that the given position is between 0–50 000 pulses and the load changes with speed. The obtained waveforms are shown in Fig. 8. Fig. 8(a) and (b) shows the waveforms of the given position, actual position, actual speed and estimated speed, respectively. It can be seen from the waveform that when the given position changes between 50 000 pulses and 0 pulses, the actual position and actual speed of the motor change with the change of the given position, the estimated speed can all vary with the change of the actual speed and the estimation performance is good.

The actual load torque and the estimated load torque obtained by the torque-speed sensor, traditional sliding mode observer, and proposed sliding mode observer are shown in Fig. 8(c). From the waveform, it can be seen that the estimated load torque varies with the change of the actual load torque, but the chattering and delay of the estimated load torque obtained by the traditional sliding mode observer are large because it does not include adaptive control. There is a significant error and delay with the actual load torque. After adding the proposed adaptive control and improvement of the cut-off frequency, the chattering and delay of the estimated load torque obtained by the proposed sliding mode observer are improved.

Therefore, comparing the above test results, it can be seen that the estimated speed of the two sliding mode observers can all follow the change of the actual speed for the speed estimation, but for the identification of load moment, the estimated load torque of the improved sliding mode observer not only has smaller error and chattering but also has better dynamic response performance, which has better estimation performance than that of the traditional sliding mode observer.

C. Test of Parameter Changes and External Disturbances

The main parameters that affect the performance of the proposed method are the resistance, direct axis inductance, quadrature axis inductance, and mechanical inertia of the motor. The influence of four parameters changes is analyzed based on the modeling and simulation methods.

Firstly, the influence of the stator resistance changes is analyzed. The rated value of resistance is 0.68Ω (Rs = 0.68 Ω). When the resistance changes to 2, 5, 0.5, and 0.2Rs, the simulation results of position, speed and load torque are, as shown in Fig. 9(a)–(c), respectively. Observing the waveforms of Fig. 9(a) and (b), we can see that when 500 pulses (as the position command) are given, the motor reaches the given position after 0.49 s, and the maximum speed of the corresponding motor is 93.34 r/min. When the position reference is changed to 0 pulses, the motor reaches the given position after 0.43 s, and the maximum speed of the corresponding motor is −93.32r/min. The actual position is slightly affected by the change in the resistance, and the maximum change of the position is 0.1 pulses due to resistance variation. The speed estimated by the sliding mode observer can well follow the actual speed change. When the resistance changes between (0.2–5)Rs, the estimated speed is less affected, and the maximum deviation is 0.03 r/min. It can be seen from the waveform of Fig. 9(c) that the given load torque is proportional to the motor speed. When the resistance changes between (0.2–5)Rs, the estimated load torque is also less affected by the change of resistance, and the maximum deviation is 0.002 N.m. According to the above analysis, the change of the resistance has little influence on the proposed sliding mode observer for load identification.

Secondly, the influence of the direct axis inductance change is analyzed. The rated value of direct axis inductance is 0.0055 mH (Ld = 0.0055 mH). When the direct axis inductance value changes to 2, 5, 0.5, and 0.2 Ld, the simulation results of position, speed and load torque are as shown in Fig. 10(a)–(c),

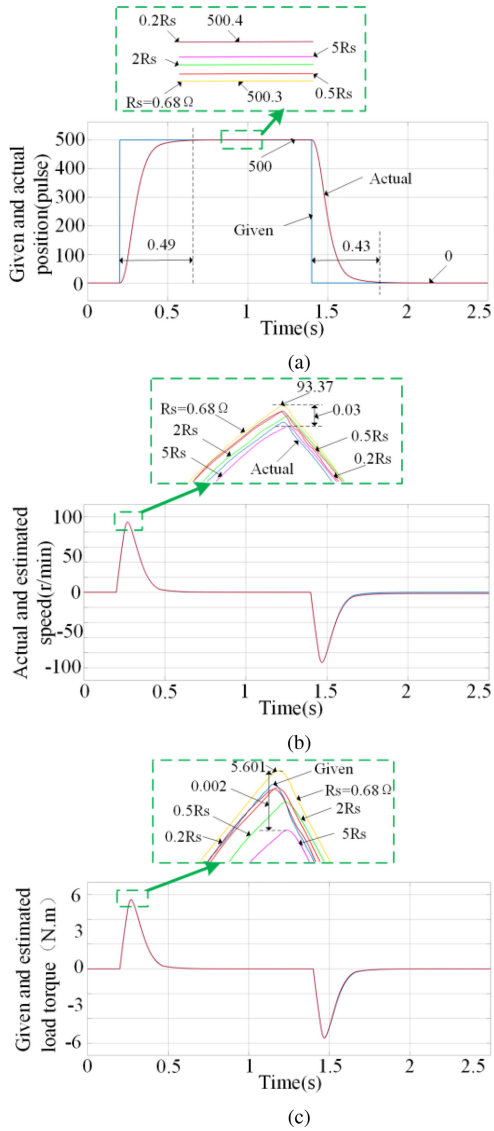

Fig. 9. Waveform of estimated speed and load torque under the different stator resistances. (a) Given and actual position. (b) Actual and estimated speed. (c) Given and estimated load torque.

respectively. Observing the waveforms of Fig. 10(a) and (b), we can see that when 500 pulses are given as the position reference, the motor reaches the given position after 0.49s, and the maximum speed of the corresponding motor is 93.33 r/min. When the position reference is changed to 0 pulses, the motor reaches the given position after 0.43 s, and the maximum speed of the corresponding motor is −93.32 r/min. The actual position is slightly affected by the change of the inductance of the direct axis, and the maximum deviation is 0.1 pulses. The speed estimated by the sliding mode observer can well follow the actual speed change. When the direct axis inductance changes between (0.2–5)Ld, the estimated speed is less affected, and the maximum deviation is 0.16 r/min. Observing the waveforms of Fig. 10(c), we can see that the given load torque is a proportional function of the motor speed. When the direct axis inductance value changes, the estimated load torque is also less affected,

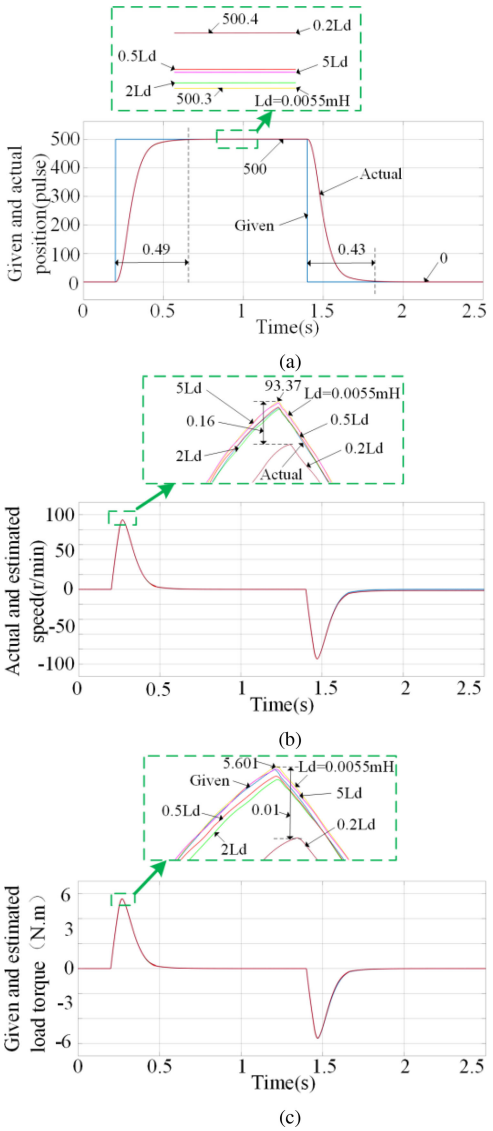

Fig. 10. Waveform of estimated speed and load torque under the different direct axis inductance. (a) Given and actual position. (b) Actual and estimated speed. (c) Given and estimated load torque.

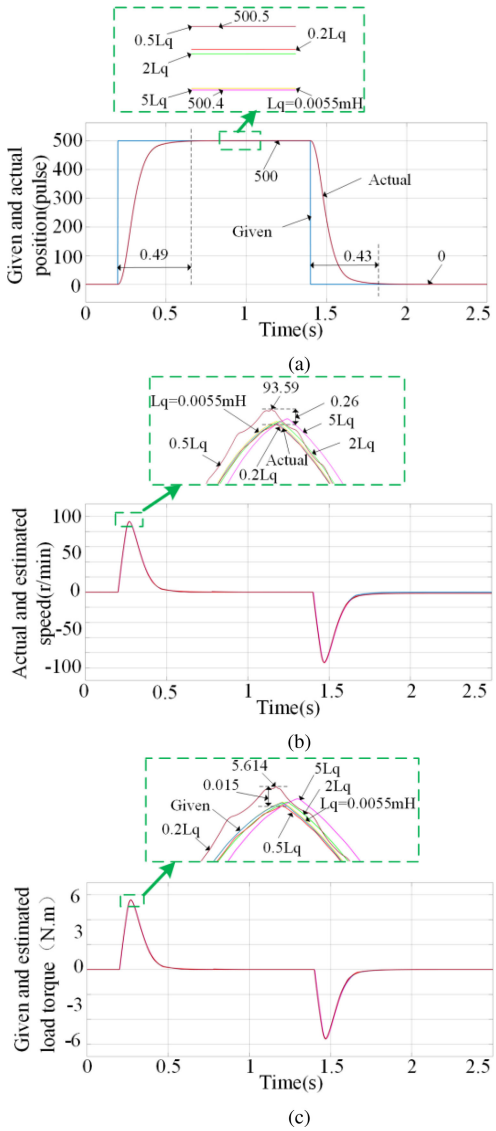

Fig. 11. Waveform of estimated speed and load torque under the different quadrature axis inductance. (a) Given and actual position. (b) Actual and estimated speed. (c) Given and estimated load torque.

and the maximum deviation is 0.01 N.m. According to the earlier analysis, the change of direct axis inductance has little influence on the proposed sliding mode observer for load identification.

Third, the influence of the change of the quadrature axis inductance is analyzed. The rated value of quadrature axis inductance is 0.0055 mH (Lq = 0.0055 mH). When the quadrature axis inductance value changes to 2, 5, 0.5, and 0.2 Lq, the simulation results of position, speed and load torque are as shown in Fig. 11(a)–(c), respectively. Observing the waveforms of Fig. 11(a) and (b), we can see that when 500 pulses are given as the position reference, the motor reaches the given position after 0.49 s, and the maximum speed of the corresponding motor is 93.37 r/min. When the position reference is changed to 0 pulses, the motor reaches the given position after 0.43 s, and the maximum speed of the corresponding motor is −93.32 r/min. The actual position is slightly affected by the change of the quadrature axis inductance value, and the maximum deviation is 0.1 pulses. The speed estimated by the sliding mode observer can well follow the actual speed change. When the quadrature axis inductance value changes between (0.2–5)Lq, the estimated speed is less affected, and the maximum deviation is 0.26 r/min. It can be seen from the waveform of Fig. 11(c) that the given load torque is proportional to the motor speed. When the quadrature axis inductance changes, the estimated load torque is also less affected, and the maximum deviation is 0.015 N.m. According to the earlier analysis, the change of quadrature axis inductance has little influence on the proposed sliding mode observer for load identification.

Finally, the influence of the change of the moment of inertia is analyzed. The rated moment of inertia of the motor is 0.01482 kg.m^2 (J = 0.01482 kg.m^2). When the moment of inertia changes to 2, 5, 0.5, and 0.2 J, the simulation results of position, speed,

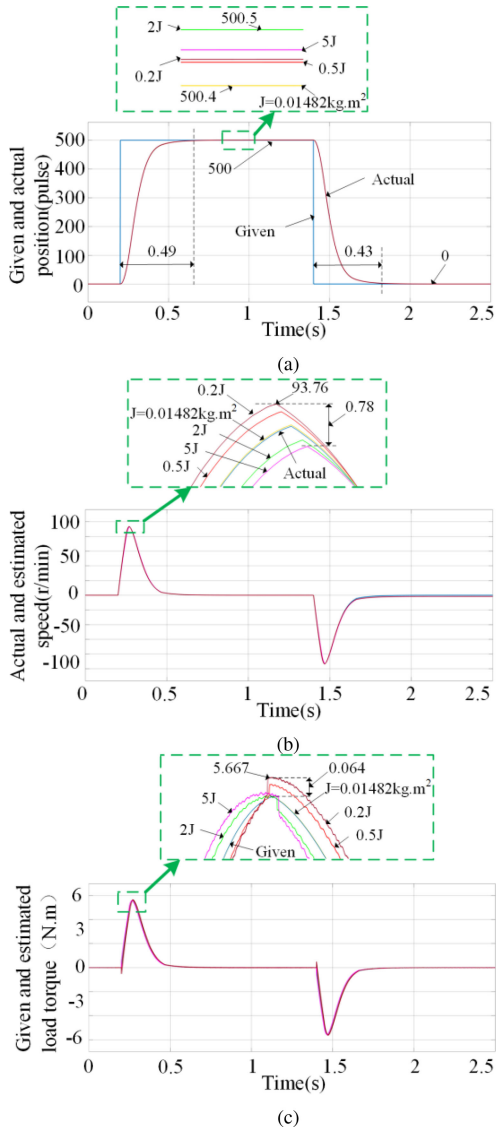

Fig. 12. Waveform of estimated speed and load torque under the different moment of inertia. (a) Given and actual position. (b) Actual and estimated speed. (c) Given and estimated load torque.

and load torque are as shown in Fig. 12(a)–(c), respectively. Observing the waveforms of Fig. 12(a) and (b), we can see that when 500 pulses are given as the position reference, the motor reaches the given position after 0.49 s, and the maximum speed of the corresponding motor is 93.38r/min. When the position reference is changed to 0 pulses, the motor reaches the given position after 0.43 s, and the maximum speed of the corresponding motor is −93.32 r/min. The actual position is slightly affected by the change of the moment of inertia, and the maximum deviation is 0.1 pulses. The speed estimated by the sliding mode observer can well follow the actual speed change. When the moment of inertia changes between (0.2–5)J, the estimated speed is less affected, and the maximum deviation is 0.78 r/min. It can be seen from the waveform of Fig. 12(c) that the given load torque is proportional to the motor speed. When the moment of inertia changes between (0–2-5) J, the estimated load torque is less affected by the change of moment of inertia and the maximum deviation is 0.064 N.m. According to the earlier analysis, the change of moment of inertia has little influence on the proposed sliding mode observer for load identification.

According to the earlier analysis, it may be concluded that the changes of resistance, direct axis inductance, quadrature axis inductance, and moment of inertia have little influence on the proposed sliding mode observer for load identification, which indicates the method has good robustness.

D. Comparative Test of the Positioning Performance

In order to verify the effectiveness of the position servo system designed by the proposed improved sliding mode observer and feed-forward compensation, as shown in Fig. 3, a comparative test is carried out in this article, under the condition that the given position is a square wave curve which changes between 0 and 1000 pulses, and the experimental waveforms of the given position, the actual position and the estimated load torque are obtained as shown in Fig. 13, respectively.

It can be seen from the waveforms that, in the first stage the designed position servo system running without load does not introduce the feed-forward compensation, the actual position of the motor rises from 0 pulses to 1000 pulses after about 0.25 s, and the positioning error is about −2 pulses. The actual position drops from 1000 pulses to 0 pulses after 0.26 s, and the positioning error is about 1.2 pulses. The load torque estimated by the proposed sliding mode observer change between −0.65 to 0.66 N.m.

In the second stage, the feed-forward compensation algorithm is not introduced, but the load is suddenly added at time $t =$ 2.8 s and the load torque estimated by the proposed sliding mode observer change between −0.74 to 0.79 N.m. There is a big error (45 pulses) occurred between the actual position and the given position, and the actual position cannot reach the given position in the same square waveform period when the given position rises from 0 pulses to the 1000 pulses. The error of 13.2 pulses and the failure to reach the given position also occur, when the given position drops from 1000 pulses to 0 pulses. Therefore, the variation of the load reduces the positioning accuracy of the motor.

In the third stage, when the system is running with load, the feed-forward compensation algorithm is introduced. According to the observation of the waveform, the actual position of the motor rises from 0 pulses to 1000 pulses after 0.34 s, and the positioning error decreases to 2 pulses. The actual position decreases from 1000 pulses to 0 pulses after 0.31 s, and the positioning error decreases to 1 pulse.

Second, another comparative test is carried out in this paper, under the condition that the given position is a square wave curve which changes between 0 and 60 000 pulses. The experimental waveforms of the given position, the actual position and the estimated load torque are obtained, as shown in Fig. 14, respectively.

It can be seen from the waveforms that, in the first stage, the designed position servo system running without load does not introduce the feed-forward compensation. The actual position of the motor rises from 0 pulses to 60 000 pulses after about

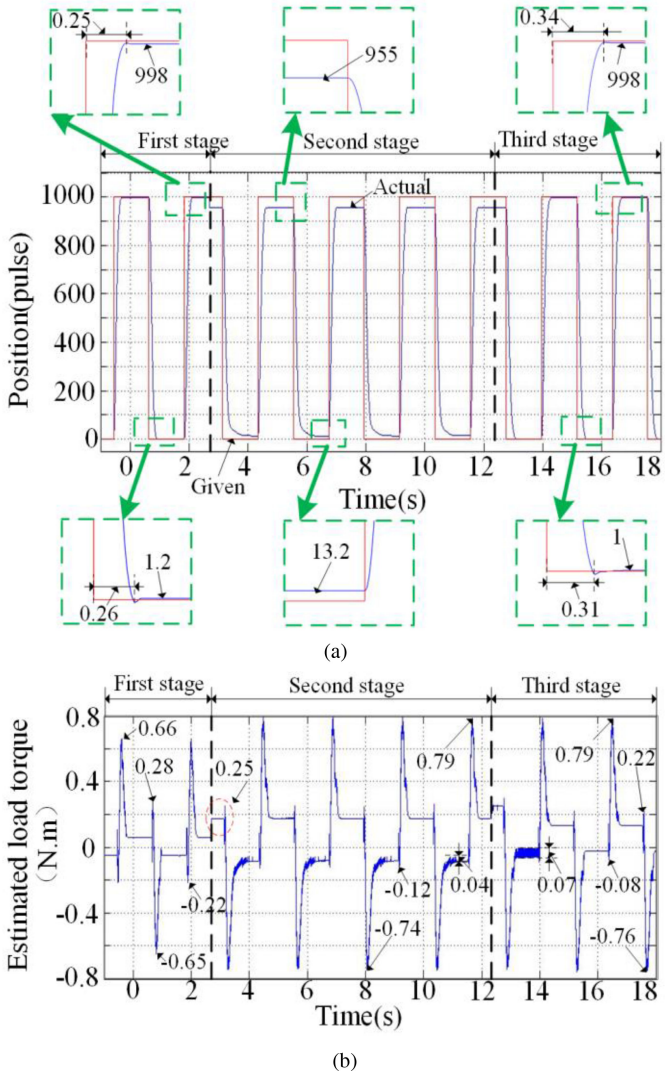

Fig. 13. Test under the condition that the given pulse is 0–1000 and the actual load is a function of speed. (a) Given and actual position. (b) Estimated load torque.

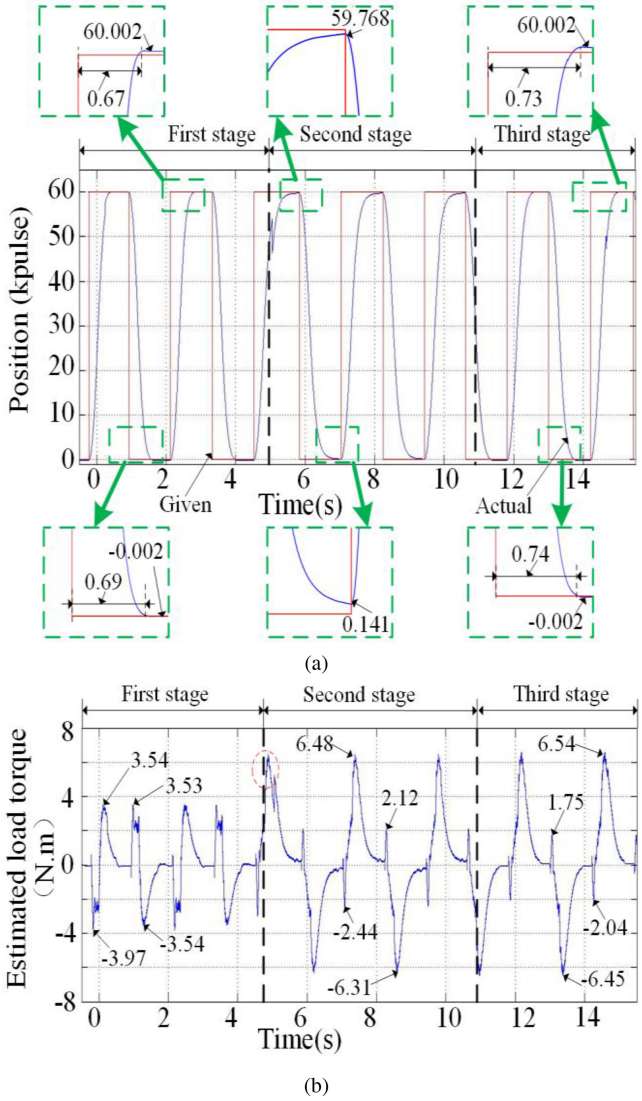

Fig. 14. Test under the condition that the given pulse is 0–60 000 and the actual load is a function of speed. (a) Given and actual position. (b) Estimated load torque.

0.67 s, and the positioning error is about 2 pulses. The actual position drops from 60 000 to 0 pulses after 0.69 s, and the positioning error is about −2 pulses. The load torque estimated by the proposed sliding mode observer change between −3.97 to 3.54 N.m.

In the second stage, the feed-forward compensation algorithm is not introduced, but the load is suddenly added at time $t = 4.8$ s and the load torque estimated by the proposed sliding mode observer change between −6.31 to 6.48 N.m. There is a big error (232 pulses) occurred between the actual and given position, and the actual position cannot reach the given position in the same square wave period when the given position rises from 0 pulses to the 60 000 pulses. The error of 141 pulses and the failure to reach the given position also occur, when the given position drops from 60 000 to 0 pulses. Therefore, the variation of the load reduces the positioning accuracy of the motor.

In the third stage, when the system is running with load, the feed-forward compensation algorithm is introduced. According to the observation of the waveform, the actual position rises from 0 pulses to 60 000 pulses after 0.73 s, and the positioning error decreases to −2 pulses. The actual position decreases from 60 000 pulses to 0 pulses after 0.74s, and the positioning error decreases to −2 pulses.

Therefore, according to the earlier experimental results, the introduction of the proposed sliding mode observer and the feed-forward compensation algorithm can improve the positioning accuracy of the position servo system.

V. Conclusion

1) Load disturbance rejection is one of the key technologies in the research and development of high-speed and high-precision position servo system. According to the design idea of "(parameter) identification-adjustment (compensation)-adaptation," a load torque self-adaptive identification sliding mode observer is proposed based

on the adaptive control and improvement of the cut-off frequency.

2) In order to verify the correctness of the scheme, the corresponding test platform is built and compared. The experimental results show that, compared with the traditional observer, the proposed improved sliding mode observer can realize the compensation of the estimation error with variable-speed or load through the adaptive adjustment of the cut-off frequency of the low-pass filter and the adaptive control of the feedback gain coefficient. Whether the load is constant or variable, the estimation accuracy of load torque is high.
3) The position servo system designed based on the proposed sliding mode observer can improve the response against load change on the system during the positioning process. It is an effective method for the high-precision positioning control of the position servo system with a variable-speed or variable-load, which provides a solution for the hybrid control of the force and position of the cooperative robot.

REFERENCES

[1] T. D. Do, S. Kwak, H. H. Choi, and J. W. Jung, "Suboptimal control scheme design for interior permanent-magnet synchronous motors: An SDRE-based approach," *IEEE Trans. Power Electron.*, vol. 29, no. 6, pp. 3020–3031, Jul. 2014.

[2] B. Du, S. Wu, and S. H, "Application of linear active disturbance rejection controller for sensorless control of internal permanent-magnet synchronous motor," *IEEE Trans. Ind. Electron.*, vol. 63, no. 5, pp. 3019–3027, May. 2016.

[3] Y. Huang and S. Xiong, "IMC-based current observer for PMSM," *Electron. Letters*, vol. 51, no. 25, pp. 2100–2102, Dec. 2015.

[4] C. Xia, Y. Yan, and P. Song, "Voltage disturbance rejection for matrix converter-based PMSM drive system using internal model control," *IEEE Trans. Ind. Electron.*, vol. 59, no. 1, pp. 361–372, Jan. 2012.

[5] J. Zhao, J. Huang, and Y. Xu, "Research of fuzzy two degree of freedom PID control for permanent magnet synchronous linear motor," in *Proc. 17th Int. Conf. Elect. Mach. Syst.*, 2014, pp. 1723–1727.

[6] Z. Pan, F. Dong, J. Zhao, L. Wang, and Y. Feng, "Combined resonant controller and two-degree-of-freedom PID Controller for PMSLM current harmonics suppression," *IEEE Trans. Ind. Electron.*, vol. 65, no. 9, pp. 7558–7568, Sep. 2018.

[7] X. Zhao, X. Huang, and Y. Xu, "Piecewise variable universe fuzzy iterative learning control for permanent magnet linear synchronous motor servo system," *Trans. China Electrotechn. Soc.*, vol. 32, no. 23, pp. 9–15, Dec. 2017.

[8] D. Flieller, N. K. Nguyen, P. Wira, and G. Sturtzer, "A Self-learning solution for torque ripple reduction for nonsinusoidal permanent-magnet motor drives based on Artificial neural networks," *IEEE Trans. Ind. Electron.*, vol. 61, no. 2, pp. 655–666, Apr. 2013.

[9] H. Chaoui, M. Khayamy, and A. A. Aljarboua, "Adaptive interval type-2 fuzzy logic control for PMSM drives with a modified reference frame," *IEEE Trans. Ind. Electron.*, vol. 64, no. 5, pp. 3786–3797, May. 2017.

[10] T. Tuovinen and sM. Hinkkanen, "Signal-Injection-Assisted Full-order observer with parameter adaptation for synchronous reluctance motor drives," *IEEE Trans. Ind. Appl.*, vol. 50, no. 5, pp. 3392–3402, Feb. 2014.

[11] W. Lu, K. Ji, H. Dong, J. Zhang, Q. Wang, and L. Guo, "Double position servo synchronous drive system based on cross-coupling integrated feedforward control for broacher," *Chin. J. Mech. Eng.*, vol. 30, no. 2, pp. 272–285, Mar. 2017.

[12] L. Sun and Z. Zheng, "Disturbance-observer-based robust backstepping attitude stabilization of spacecraft under input saturation and measurement uncertainty," *IEEE Trans. Ind. Electron.*, vol. 64, no. 10, pp. 7994–8002, Apr. 2017.

[13] X. Zhang, B. Hou, and Y. Mei, "Deadbeat predictive current control of permanent-magnet synchronous motors with stator current and disturbance observer," *IEEE Trans. Power Electron.*, vol. 32, no. 5, pp. 3818–3834, May. 2017.

[14] T. Shi, Z. Wang, and C. Xia, "Speed measurement error suppression for PMSM control system using self-adaption kalman observer," *IEEE Trans. Ind. Electron.*, vol. 62, no. 5, pp. 2753–2763, Oct. 2014.

[15] G. Feng, C. Lai, J. Tjong, N. Kar, "Non-invasive Kalman filter based permanent magnet temperature estimation for permanent magnet synchronous machines," *IEEE Transa. Power Electron.*, vol. 1, no. 1, pp. 1–9, Feb. 2018.

[16] Y. Mei, K. Sun, and Y. Shi, "A 2-D fuzzy logic based MRAS scheme for sensorless control of interior permanent magnet synchronous motor drives with cyclic fluctuating loads," *Chin. J. Elect. Eng.*, vol. 1, no. 1, pp. 85–91, Dec. 2015.

[17] M. L. Masmoudi, E. Etien, S. Moreau, and A. Sakout, "Amplification of single mechanical fault signatures using full adaptive PMSM observer," *IEEE Trans. Ind. Electron.*, vol. 64, no. 1, pp. 615–623, Jan. 2017.

[18] D. Xu, T. Wang, and H. Wei, "Inertia identification and error compensation of permanent magnet synchronous motor based on simplified model," *Trans. China Electrotechn. Soc.*, vol. 28, no. 2, pp. 126–131, Feb. 2013.

[19] H. Ji, S. Wang, and S. Wang, "Research on adaptive identification method of moment of inertia for permanent magnet synchronous motor," *J. Huazhong Univ. Sci. Technol*, vol. 43, no. 1, pp. 122–126, Nov. 2015.

[20] T. Chen, J. Zhang, and Y. Peng, "Load disturbance control method based on torque sliding mode observer," *Power Syst. Protection Control*, vol. 41, no. 8, pp. 114–118, Jul. 2013.

[21] Wenqi Lu *et al.*, "A new load torque identification sliding mode observer for permanent magnet synchronous machine drive system," *IEEE Trans. Power Electron.*, vol.34, no. 8, pp. 7852–7862, Aug. 2019.

Wenqi Lu received the B.S. degree from Zhejiang Ocean University, Zhejiang, China, in 2005, and the Ph.D. degree from the Nanjing University of Aeronautics and Astronautics, Nanjing, China, in 2011.

From 2014 to 2017, he was a Postdoctoral Researcher with the Department of Electrical Engineering, Zhejiang University. From 2017 to 2018, he was a Guest Researcher with the Department of Energy Technology, Aalborg University. He is currently an Associate Professor with the Faculty of Mechanical Engineering and Automation, Zhejiang Sci-Tech University. His current research interests include the control of electric machines and mechatronic system and its application in robot and intelligent manufacturing equipment.

Bo Tang received the B.S. degree in mechanical and electrical engineering from Chongqing University of Science and Technology, Chongqing, China, in 2019. He is currently working toward the master's degree in mechanical and electrical engineering with Zhejiang Sci-Tech University, Zhejiang, China.

His research interests include design of electrical motor drives, and control of permanent magnet synchronous motors.

Kehui Ji received the B.S. degree in electrical engineering from JiangSu University, Zhenjiang, China, in 2001, and the M.S. and Ph.D. degrees from Zhejiang University, Hangzhou, China, in 2004 and 2013, respectively, all in electrical engineering.

From 2004 to 2010, he worked in industry, as an R&D Engineer, working principally on the design of the permanent magnet machine and drive. Since 2013, he has been a Lecturer with Zhejiang Sci-Tech University, Hangzhou, China. His research interests include electrical machine drives and motion control systems.

Kaiyuan Lu (Member, IEEE) received the B.S. and M.S. degrees from Zhejiang University, Zhejiang, China, in 1997 and 2000, respectively, and the Ph.D. degree from Aalborg University, Aalborg, Denmark, in 2005, all in electrical engineering.

In 2005, he was an Assistance Professor with the Department of Energy Technology, Aalborg University, where he has been an Associate Professor since 2008. His research interests include design of permanent magnet machines, finite element method analysis, and control of permanent magnet machines.

Dong Wang (Member, IEEE) received the B.S. degree from Zhejiang University, Zhejiang, China, in 2004, and the M.S. and Ph.D. degrees from Aalborg University, Denmark, in 2006 and 2016, respectively, all in electrical engineering.

From 2006 to 2012, he was with Grundfos R&D China, Suzhou, China, as a Senior Motor Engineer, working on the design and analysis of the permanent magnet machine and devices. From 2016 to 2017, he was a Postdoc Researcher with the Department of Energy Technology, Aalborg University, where he has been an Assistant Professor since 2017. His research interests include design and control of synchronous reluctance and permanent magnet machines.

Zhijun Yu received the B.S. degree from Nanjing Agricultural University, Nanjing, China, in 2006, and the M.S. degree from Naval Engineering University, Wuhan, China, in 2011.

Since 2013, he was a General Manager with the Jiangsu Yuandong Electric Manufacturing Co., Ltd., Taizhou, Jiangsu Province, China, working on the design and analysis of the permanent magnet machine and devices. His research interests include the design of permanent magnet machines, FEM analysis, and control of permanent magnet machines.